

# Proposed SMA Tension Sling Damper for Passive Seismic Control of Building

S. H. Mehta & S. P. Purohit

*Department of Civil Engineering, School of Engineering, Institute of Technology, Nirma University, Ahmedabad, Gujarat, India - 382481*

**ABSTRACT:** Passive Shape Memory Alloy (SMA) based Tension Sling Damper (TSD) is proposed to control seismic response of building represented as dynamic SDOF system. Non-linear hysteretic behavior of SMA is characterized by Tanaka model with seismic excitations as input. It is converted to equivalent piece-wise linear elastic viscous damping model described by stiffness constant ' $k_{eff}$ ' and damping constant ' $c_{eff}$ ' to implement it with linear dynamic system. Damping constant ' $c_{eff}$ ' is evaluated for TSD for given seismic excitation at each instance of time defined as instantaneous damping, unlike constant damping used in other studies, to derive accurate seismic response of the dynamic system. Seismic response control parameters – peak and rms performance indices (PI) for displacement and acceleration, peak damper force, maximum damping ratio are evaluated for flexible, moderately stiff and stiff dynamic systems fitted with TSD under pulse and strong ground motion type seismic excitations with varied PGA. Substantial reduction in PI is observed for controlled systems through varying design parameters of TSD – cross-sectional area and length of SMA sling. TSD yields better seismic response control for moderately stiff and flexible system due to super-elastic properties of SMA. Further, it works efficiently for seismic excitations with low to moderate PGA.

## 1 INTRODUCTION

Seismic response control of structure has been extremely important to safeguard it from excessive damage. Passive energy dissipation systems for seismic application have received much attention since mid-1990s as these require no external power to attenuate damage to the framing system. Passive damping devices include viscous fluid damper, viscoelastic damper, metallic damper, friction damper etc. (Symans et al. 2008). It has been realized that such devices yield limited structural response control due to inability of the damper to respond in real time. This leads to development of semi-active dampers capable of modifying its mechanical properties with real time (Soong et al. 2002, Spencer et al. 2003). Most common among semi-active dampers are Electrorheological and Magnetorheological dampers (Xu et al. 2000) that are used to produce actuation force estimated through Optimal Control Theories (Jansen & Dyke 1999, Purohit & Chandiramani 2010). Following the success of semi-active dampers, post 2000 have seen many active dampers and dampers with combination of active and passive elements (hybrid dampers) developed to control seismic response of the structure. Since, both, semi-active and active dampers use damping materials with unique controllable properties in real time, there has been a surge in active research to explore such materials in last decade. Recently, Shape Memory Alloys (SMA) have drawn significant attention for potential seismic application

in structures due to their unique and superior properties of phase transformations. Typical SMA exists in two different phases - martensite & austenite with their reversible transformation being stress or temperature dependent (Buehler & Wiley, 1961).

The unique characteristics of Cu-Zn and Cu-Al alloys to undergo reversible thermo-elastic martensitic transformation had been demonstrated first by Kurdjumov & Khandros (1949). In 1963, Buehler and co-workers discovered NiTi SMA at Naval Ordnance Laboratory (NOL) undergoing phase transformations offering potential to commercialize SMA applications. NitiNOL has been used in diversified fields like Automobile, Aerospace, Robotics and Biomedical (Jani et al. 2014). Song et al. (2006) have studied potential application of SMA based passive control device for seismic response control of the structure. Bertrand et al. (2013) have shown increased damping due to phase transformation from austenite to martensite when used as damper in structures. SMA based passive dampers have been developed and implemented with Reinforced Concrete frames (Dolce et al. 2005, McCormick et al. 2006); with steel frames (Mortazavi et al. 2013) and as Buckling Restrained Braces with steel frames (Miller et al. 2012). Zhang & Zhu (2007), Morais et al. (2017), in their studies, established that damping offered by SMA damper is a function of SMA wire diameter, strain rate & amplitude and pre-straining of SMA wire.

Many researchers have carried out experimental studies to understand the hysteretic behavior of SMA

material in the form of wire/rod. Caughey (1960) has represented hysteretic behavior of SMA observed under cyclic sinusoidal loading as a bilinear curve. Tanaka (1986) represented one dimensional hysteretic model for SMA which is versatile and simpler to use. Graesser & Cozzareli (1991) have included macroscopic characteristics of SMA to the existing one dimensional hysteresis model. However, prediction using G-C model drifts from experimental results of hysteretic behavior due to use of identical parameters for loading and unloading path of the model. Ren et al. (2007) have improved classical G-C model setting model parameters different for loading and unloading path to match prediction and experimental results of hysteretic behavior of SMA. Further, effect of strain rate and strain amplitude on hysteretic behavior of SMA under cyclic loading also have been studied. Experimental studies conducted by DesRoches et al. (2004) have found that damping potential of super-elastic SMA wire/bar is low and of the order less than 7% equivalent viscous damping. It has been observed that damping of SMA degrades with cyclic strain exceeding 6%. Increment in seismic loading rate observes reduction in equivalent damping in SMA, also reported by Ren et al., (2007). Energy dissipation in each cycle (Iterative Response Spectrum) of SMA has been modelled as equivalent viscous damping for sinusoidal loading (Parulekar et al. 2014). SMA wire based damper and re-centering devices for seismic response control of structures have been explored by Han et al. (2003), Zhang & Zhu (2007) and Lobo et al. (2015). Ghodke & Jangid (2016) have used SMA wire with base isolators for seismic response control of irregular building. Equivalent linear elastic viscous damping model for SMA wire has been proposed for nonlinear force deformation behavior of the isolator following AASHTO guidelines. Two model parameters, i.e. effective elastic stiffness and effective viscous damping have been derived, to map hysteretic parameters used for classical G-C model and model proposed by Ren et al. (2007).

Present paper aims to control seismic response of building modelled as SDOF dynamic system, passively, through proposed SMA based Tension Sling Damper (TSD). SDOF system fitted with TSD is subjected to various seismic excitations ranging between with low to high PGA representing pulse type and strong ground motion type. Design parameters for SMA based TSD include cross-sectional area and length of SMA sling. Maximum strain induced in SMA sling of TSD is restricted (< 6%) to eliminate non-recoverable drift of the dynamic system. Nonlinear hysteretic behavior of SMA represented by Tanaka model (Tanaka 1986) is characterized under seismic inputs. It is modelled as equivalent piece-

wise linear elastic viscous damping model to implement with linear dynamic system.

The present study has two distinct objectives to be met with; (i) to develop a reusable super-elastic SMA wire based passive damper, inducing tension forces only, to control seismic response of the building. (ii) to propose equivalent piece-wise linear elastic viscous damping model that allows evaluation of damping at each instant leading to realistic seismic control of the building. Seismic response control of the dynamic system is quantified with peak and RMS Performance Indices (PI) for displacement and acceleration under different type of seismic excitations. Damper force and damping offered by TSD at each instant are evaluated to assess efficacy for seismic response control of dynamic system.

## 2 SYSTEM MODEL

### 2.1 Tension Sling Damper (TSD)

The proposed Tension Sling Damper (TSD) uses SMA wires, bearing only tensile strain, when subjected to seismic excitations. It can be fitted at the centre/off-centre in principal diagonal member of a building frame. Figure 1a, b show schematic diagram of elevation & plan and isometric view of the damper. TSD has a rigid core box that can move freely inside the slit provided in plates connected with flanges of designated I section forming bottom bracing element. Connecting plates also house rigid rod, each at above and below rigid core box at a distance that satisfies length requirement of SMA sling as shown in Figure 1a, b. SMA slings, number as per design, are firmly attached to the rigid core box and the same are wound around rigid rod. Rigid core box receives an input motion from top bracing element (I section) as it is connected to connecting plate at the central shaft of rigid core box. It is followed that, at any instant of seismic excitation input, only one set of SMA slings wound around rigid rod is strained due to tension. At the same time, the other set of SMA slings disengages itself from the rigid rod until the direction of input changes. Smooth relative motion of the rigid core box inside the slits of connecting plates with bottom bracing element is ensured through tolerances and friction reducing agents.

Proposed TSD distinguishes itself from conventional X-bracing elements as former eliminates compression diagonal member likely to undergo buckling due to seismic excitation. Proposed passive TSD offers flexibility in design, at par, with other well established passive damping devices as: i) damper force of TSD can be tuned to input seismic excitations as designer can vary cross-sectional area and/or nos. of

SMA sling; ii) length of SMA sling can be designed without overshooting non-recoverable tensile strain limit of 0.06 strain (DesRoches et al. 2004); and iii) elimination of compressive force of the TSD prevents buckling possibility.

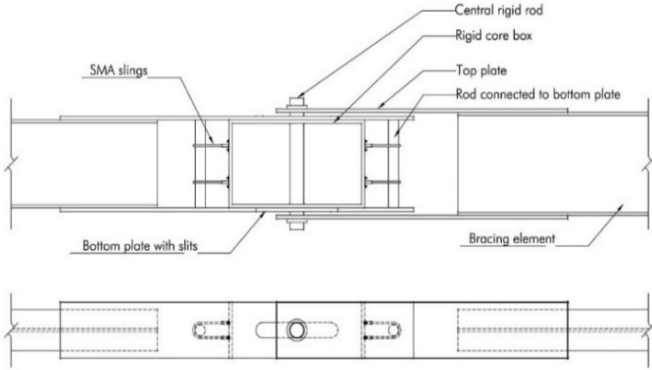


Figure 1 (a) Plan and elevation of proposed Tension Sling Damper

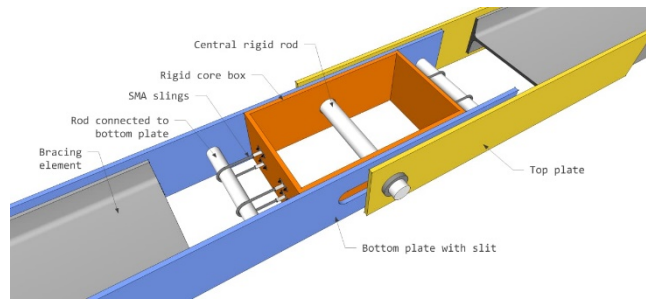


Figure 1 (b) Isometric view of proposed Tension Sling Damper

## 2.2 SMA Slings

SMA slings of the present study are characterized by unified Tanaka Model under cyclic loading leading to hysteretic stress-strain relationship. Mechanical properties (Hardtl & Lagoudas, 2008) used are : Modulus of Elasticity in Martensite ( $E_M$ ) and Austenite ( $E_A$ ) : 46 GPa and 55 GPa; Martensite Start Temperature ( $M_s$ ) and Finish Temperature ( $M_f$ ) :  $-28^\circ\text{C}$  and  $-43^\circ\text{C}$ ; Austenite Start Temperature ( $A_s$ ) and Finish Temperature ( $A_f$ ) :  $-3^\circ\text{C}$  and  $7^\circ\text{C}$ ; Stiffness influence coefficients for Martensite ( $C_M$ ) and Austenite ( $C_A$ ) : 7.4 Mpa/ $^\circ\text{C}$ ; Maximum transformation strain ( $H^{cur}(\sigma) = H_{max}$ ): 0.06. A good agreement between experimental investigation and simulated response using above properties of SMA wire has been established by Hardtl & Lagoudas (2008). The total strain in SMA sling by unified Tanaka model is expressed through Equation (1) to Equation (3).

$$\varepsilon = \varepsilon_{Elastic} + \varepsilon_{Transformation} + \varepsilon_{Thermodynamic} \quad (1)$$

$$\varepsilon_{thermodynamic} = \alpha(T - T_0) \quad (2)$$

where  $\alpha$  = co-efficient of thermal expansion,  $T$ =Temperature of SMA element at that instant and  $T_0$ =Initial temperature

$$\varepsilon_{Transformation} = \xi H^{cur}(\sigma) \quad (3)$$

where  $\xi$  = % of martensite by volume and  $H^{cur}(\sigma)$  = maximum transformation strain.

Loading/unloading or heating/cooling of SMA slings induce phase transformation which is represented by parameter ' $\xi$ ', i.e., % martensite volume fraction which is a function of temperature and stress influence co-efficient. Details can be referred from Hardtl & Lagoudas (2008). Martensite volume fraction ( $\xi$ ) during phase transformation of SMA sling subjected to loading/unloading or temperature variation can be evaluated through Equation (4) to Equation (7).

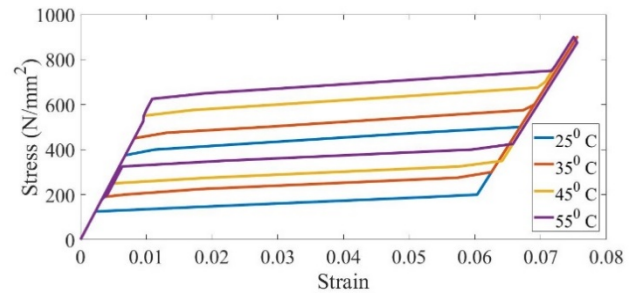


Figure 2 Variation of stress vs strain for SMA wire subjected to stress cycle at various ambient temperatures

$$\xi = 0; \text{ if } T \geq M_s^\sigma \text{ or } T \geq A_f^\sigma \quad (4)$$

$$\xi = \frac{(M_s^\sigma - T)}{(M_s - M_f)}; \text{ if } M_f^\sigma < T < M_s^\sigma \quad (5)$$

$$\xi = \frac{(A_f^\sigma - T)}{(A_f - A_s)}; \text{ if } A_s^\sigma < T < A_f^\sigma \quad (6)$$

$$\xi = 1; \text{ if } T \leq M_f^\sigma \text{ or } T \leq A_s^\sigma \quad (7)$$

where

$$A_s^\sigma = A_s + \frac{\sigma}{C_A}; \quad A_f^\sigma = A_f + \frac{\sigma}{C_M};$$

$$M_s^\sigma = M_s + \frac{\sigma}{C_M}; \quad M_f^\sigma = M_f + \frac{\sigma}{C_M}$$

Here  $A_s$ ,  $A_f$  and  $M_s$ ,  $M_f$  are start and finish temperatures while  $C_A$  and  $C_M$  are stress influence coefficients for austenite and martensite, respectively.

The elastic strain for SMA sling, thus, can be derived from Equation (1), using Equation (2) and Equation (3), given as

$$\varepsilon_{elastic} = \varepsilon - \xi H^{cur}(\sigma) - \alpha(T - T_0) \quad (8)$$

The elastic stress in SMA sling can be computed using modulus of elasticity of SMA at any instant as defined by

$$E = E_A + \xi (E_M - E_A) \quad (9)$$

where,  $E_A$  = Elastic modulus of austenite and  $E_M$  = Elastic modulus of martensite

Thus, stress in the SMA sling corresponding to given strain level for isothermal process is as follows,

$$\sigma = [E_A + \xi(E_M - E_A)] [\varepsilon - \xi H^{cur}(\sigma)] \quad (10)$$

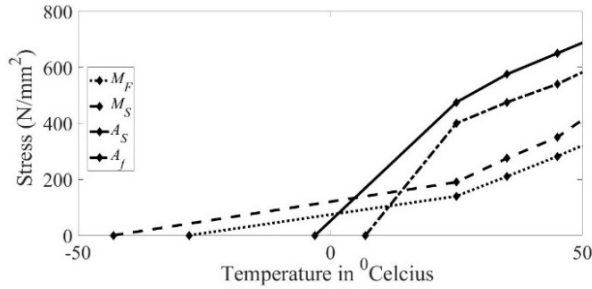


Figure 3 Stress vs transformation temperature for SMA slings

Stress-strain relationship for SMA sling given by Equation (10) is plotted in Figure 2, considering an isothermal process, for realizable ambient temperatures. Experimental studies by Hardtl & Lagoudas (2008) revealed that stress-strain relationship is well depicted by Tanaka model. Figure 3 shows relationship between stress vs transformation temperature. It is evident that increment in applied stress brings transformation temperature within the vicinity of ambient temperature range and thus SMA sling is effectively utilized as damping. This may be one of the reasons for advocating pre-strain in SMA wires by some researchers (Zhang & Zhu, 2007). Low stress levels applied to SMA sling see phase transformation at lower temperature. However, effectiveness of SMA for seismic response control at low ambient temperature is relatively less explored in literature.

### 2.3 Proposed Equivalent Piece-wise Linear Elastic Viscous Damping Model of SMA

SMA characterization studies of Tanaka, Graessar & Cozzaerelli and Ren et al establishes that hysteretic behavior comprises of nonlinear force deformation relationship. Such models find difficulties in implementation with linear dynamic system and warrants stochastic linearization method to obtain equivalent stiffness and damping (Gur et al. 2016). Further, application of SMA in base isolator for irregular building by Ghodke & Jangid (2016), following AASHTO guidelines, proposes nonlinear force deformation behavior to be modelled as equivalent linear model. The proposed model has two parameters; i) effective equivalent linear elastic stiffness and ii) effective

equivalent linear viscous damping. Therefore, characteristic linear force in the SMA wire can be represented as Equation (11).

$$F_{SMA} = k_{eff} x(t) + c_{eff} \dot{x}(t) \quad (11)$$

where  $x$ ,  $\dot{x}$  are displacement and velocity of the SMA wire respectively. Referring Fig. 3  $k_{eff}$  is given as Equation (12)

$$k_{eff} = \frac{(F_{max} - F_{min})}{(x_{max} - x_{min})} \quad (12)$$

$F_{max}$  and  $F_{min}$  are maximum and minimum forces observed by the SMA wire, where as  $x_{max}$  and  $x_{min}$  are corresponding maximum and minimum displacements.

Effective damping ratio  $\xi_{eff}$  can be determined using Figure 4 as,

$$\xi_{eff} = \frac{2 \lambda F_{ys} (x_{max} - x_y)}{2 \pi k_{eff} x_{max}^2} \quad (13)$$

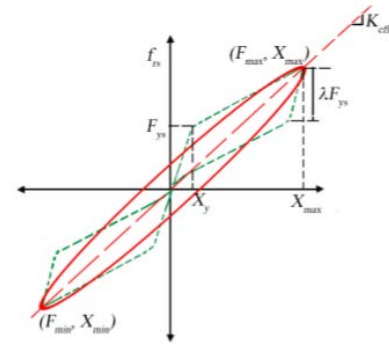


Figure 4 Equivalent stiffness for SMA wire as per AASHTO guidelines, Ghodke & Jangid (2016)

where  $\lambda F_{ys}$  is the shear force difference between the two transformation related to loading and unloading,  $\lambda = (1 - \alpha_s)$ ,  $\alpha_s$  is the ratio of transformation stiffness,  $x_y$  is the displacement corresponding to yield force of SMA wire and effective damping co-efficient  $c_{eff} = 2 * \xi_{eff} * \sqrt{k_{eff} * m}$  with usual notations.

It is evident that, SMA wire subjected to random excitations like earthquake imposes varied damping demand on SMA, unlike constant damping demand defined in Equation (13) by Ghodke & Jangid (2016).

In the present study, SMA wire represented by Tanaka model is excited under Kobe (N-S component 1964) ground motion. Nonlinear force deformation behavior of SMA wire is determined and is shown in Figure 5. Equivalent stiffness,  $k_{eff}$  as defined by Equation (12) and given by Figure 4 is evaluated for Figure 5. However, varied seismic demand of SMA wire as defined by instantaneous damping is evaluated replacing maximum displacement  $x_{max}$  of Figure 4 by

instantaneous displacement  $x_i$  in Equation (13). The instantaneous damping ratio can be expressed as Equation (14)

$$\xi_{eff}(i) = \frac{2 \lambda F_{ys} (x_i - x_y)}{2\pi * k_{eff} * x_{max}^2} \quad (14)$$

Instantaneous damping co-efficient is evaluated as,

$$c_{eff}(i) = 2 \xi_{eff}(i) \sqrt{k_{eff} * m} \quad (15)$$

SMA force generated at each instance of time due to equivalent linear constant stiffness and instantaneous damping can be expressed as

$$F_{SMA}(i) = k_{eff}x(i) + c_{eff}(i)\dot{x}(i) \quad (16)$$

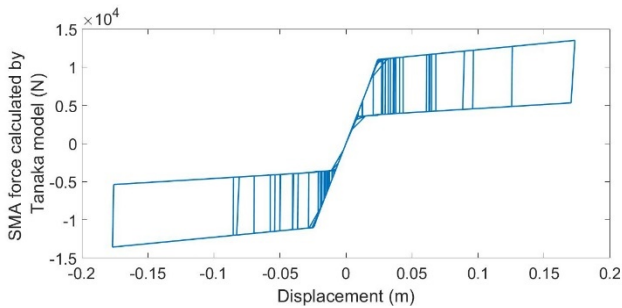


Figure 5 SMA damper force for Kobe ground displacement by unified Tanaka model

Figure 6 shows equivalent linear force deformation behavior of SMA wire under Kobe ground motion following piecewise linear equivalent elastic viscous damping based on Equation (12), Equation (14) and Equation (15).

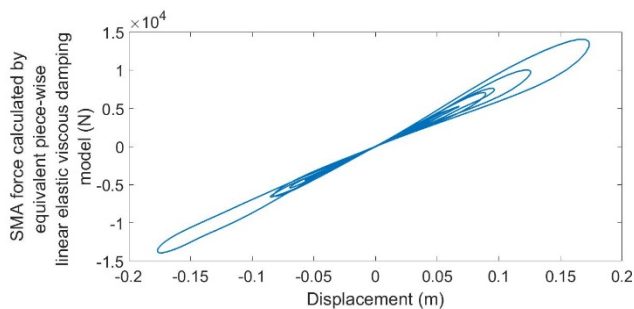


Figure 6 SMA damper force vs Kobe ground displacement represented by equivalent piece-wise linear elastic viscous damping model

Above results indicate good agreement between peak damper force derived by Tanaka model and equivalent piece-wise linear elastic viscous damping model proposed in present study. Damping component evaluated by equivalent linear elastic viscous damping model (Ghodke & Jangid, 2016) and equivalent piece-wise linear elastic viscous damping model under Kobe seismic excitations are as shown in Figure

7 and Figure 8. The apparent difference in force vs displacement relationship is due to the fact that the former (Fig. 7) uses constant stiffness and damping irrespective of seismic input received by SMA while the later (Fig. 8) evaluates damping co-efficient ‘ $c_{eff}$ ’ at each instance of time for each seismic input. This approach of SMA modelling will allow one to use compatible semi-active or active control device to further improve seismic response control of the dynamic system which is not in the scope of present study.

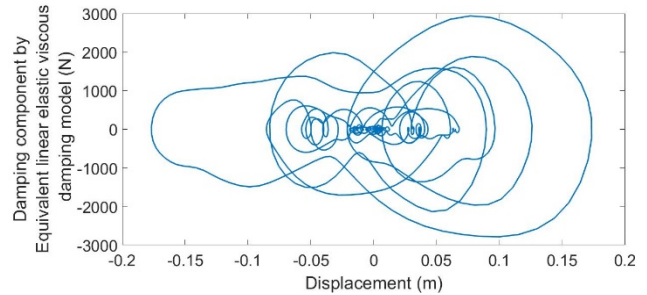


Figure 7 Force vs displacement relationship for equivalent linear elastic viscous damping model of SMA to Kobe seismic excitation

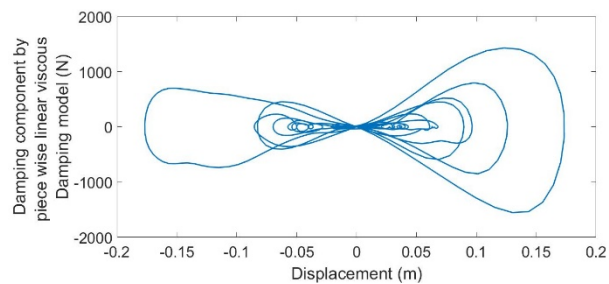
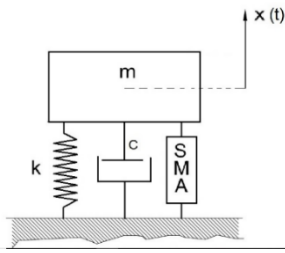


Figure 8 Force vs displacement relationship for equivalent piece-wise linear elastic viscous damping model of SMA to Kobe seismic excitation

## 2.4 Structural Model

A building modelled as discrete linear Single Degree of Freedom (SDOF) system with dominant flexural mode of vibration is considered as shown in Figure 9. Dynamic properties of the system considered are  $k/m = 17.55 /s^2$ ;  $c/m = 0.084 /s$  and  $\xi = 0.01$  (Seelecke et al. 2002). Seismic excitations representing pulse type earthquake – Loma Prieta 1989 (PGA-0.64g, E-W component) & Kobe 1964 (PGA-0.829g, N-S component) and strong motion earthquakes – Taft 1952 (PGA-0.179g, E-W component) & El Centro 1945 (PGA-0.29g, N-S component) are used in the present study. These excitations are padded with zero acceleration data appropriately to ensure decaying seismic response of the SDOF system.

Passive TSD, developed in Section 2.1, is attached to the SDOF system and schematically shown in Figure 9. Design parameters of TSD – cross-sectional



area (diameter) and length of SMA slings are evolved to achieve desirable seismic response control. These

Figure 9 Discrete mathematical model of SDOF system with Tension Sling Damper

design parameters are determined imposing constraint on strain limit to negate residual strain of TSD.

Dynamic equilibrium equation of motion for the linear SDOF system with TSD subjected to seismic excitation is expressed as

$$m\ddot{x}(t) + c\dot{x}(t) + kx(t) + F_{SMA}(t) = -m\ddot{x}_g(t) \quad (17)$$

where  $m$ ,  $k$  and  $c$  are mass, stiffness and damping coefficient;  $\ddot{x}_g$  is seismic ground acceleration and  $F_{SMA}$  is the passive damping force exerted by the TSD. As non-linear passive damper force  $F_{SMA}$  given by Tanaka model is represented by equivalent piecewise linear elastic viscous damping model, defined by Equation (16) introduced in Section 2.3, dynamic equation of motion (Equation (17)) is modified to

$$m\ddot{x}(t) + (c+c_{eff}(i)) \dot{x}(t) + (k+k_{eff}) x(t) = -m\ddot{x}_g(t) \quad (18)$$

### 3 RESULTS AND DISCUSSION

Uncontrolled displacement response of SDOF system under Taft seismic excitation is extracted as shown in Figure 10a to validate it with results by Seelecke et al (2002) reproduced in Figure 10b. Comparison of response shows good agreement to miniscule extent.

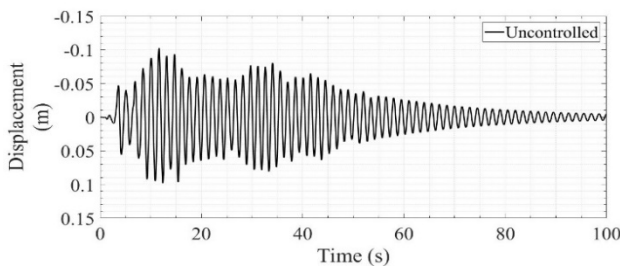
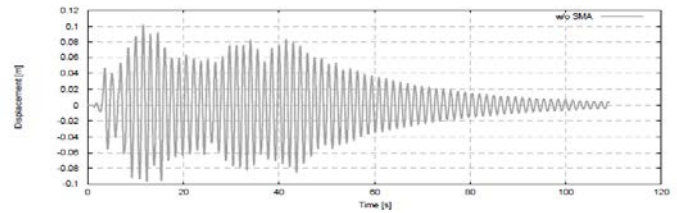


Figure 10a Uncontrolled displacement response of SDOF System subjected to Taft seismic excitation (present study)  
Figure 10 b Uncontrolled displacement response of SDOF system subjected to Taft seismic excitation (Seelecke et al. 2002)

Seismic response parameters of controlled SDOF system with TSD are defined through peak and rms Performance Indices (PI) (Ohtori et al. 2004), with usual notations in Table 1.

Peak and rms PI for displacement and acceleration responses, peak damper force, maximum strain and peak instantaneous damping ratio are evaluated for three types of dynamic systems - flexible system ( $T_n=1.5s$ ); moderately stiff system ( $T_n=0.7s$ ); stiff system ( $T_n=0.3s$ ) fitted with TSD subjected to seismic



excitations.

Table 1. Peak and rms performance indices (PI) for Controlled SDOF System

Peak Displacement	RMS Displacement
$J_1 = \frac{\max  x_{controlled} }{\max  x_{uncontrolled} }$	$J_2 = \frac{\text{rms}  x_{controlled} }{\text{rms}  x_{uncontrolled} }$
Peak Acceleration	RMS Acceleration
$J_3 = \frac{\max  \ddot{x}_{controlled} }{\max  \ddot{x}_{uncontrolled} }$	$J_4 = \frac{\text{rms}  \ddot{x}_{controlled} }{\text{rms}  \ddot{x}_{uncontrolled} }$

Design parameters – cross-sectional area (diameter and nos of SMA slings) and sling length are evaluated to control seismic response of the dynamic system. Iterative simulations to derive unified design parameters are attempted for three dynamic systems under each seismic excitation. Seismic response parameters reported in Table 2 show mostly considerable reduction for peak and rms displacement and acceleration response. As flexible dynamic system undergoes large displacement relative to other two dynamic systems, such system warrants relatively higher sling length to keep strain within 6% of limiting for super-elastic SMA. It is seen that unified design parameters for each seismic excitation yields much lower maximum strain then limiting strain of 6% for moderately stiff and stiff dynamic systems.

It is evident from Table 2 that controlled SDOF system with TSD yields substantial reduction in peak and rms PI for pulse type seismic excitation with strain values of about 4 to 4.5%. On similar lines, controlled SDOF system with TSD yields considerable reduction in peak and rms PI for strong motion type seismic excitations – El Centro, however, such results for peak and rms PI under Taft excitation are achieved when maximum strain in SMA wire is of the order of 6% .

Revised Table 2. Seismic response parameters- peak and rms PI, peak damper force and maximum damper force of controlled SDOF systems under seismic excitation

Time Histories	Time Period, $T_h$ (s)	TSD Design Parameters		Performance Indices (PI)				Maximum Strain	Peak Damper Force (kN)	Peak Instantaneous Damping Ratio (%)
		Nos. of Tension Slings (6 mm dia)	Sling length h (m)	$J_1$	$J_2$	$J_3$	$J_4$			
Taft (0.173g)	1.5	1	1.125	0.692	0.495	0.886	0.566	0.058	104.30	22.08
	0.7	1	1.125	0.920	0.861	0.986	0.835	0.030	45.951	10.08
	0.3	1	1.125	0.833	0.747	0.825	0.739	0.011	7.848	1.98
Kobe (0.829g)	1.5	6	7.6	0.784	0.580	0.829	0.651	0.060	701.811	8.98
	0.7	6	7.6	0.728	0.588	0.798	0.593	0.042	552.190	6.00
	0.3	6	7.6	0.976	0.872	0.964	0.839	0.005	42.701	0.00
Loma Prieta (0.64g)	1.5	1	4.4	0.900	0.644	1.000	0.761	0.028	53.529	3.26
	0.7	1	4.4	0.752	0.608	0.798	0.610	0.041	126.26	5.28
	0.3	1	4.4	0.913	0.798	0.939	0.794	0.013	24.734	1.00
El Centro (0.289g)	1.5	1	2.2	0.855	0.565	0.996	0.665	0.047	85.717	6.57
	0.7	1	2.2	0.805	0.703	0.886	0.726	0.034	70.363	4.51
	0.3	1	2.2	0.912	0.688	0.995	0.684	0.008	11.197	0.28

It has been found that seismic excitations bearing relatively low PGA (Taft, Loma Prieta and El Centro), are well resisted by SMA based TSD comprising of 6 mm diameter single tension sling of varied sling length. However, nos. of tension slings increases to 6 with higher length of sling for TSD to resist seismic excitation of high PGA (Kobe). It is realized that both design parameters such as diameter and length of tension sling play an important role in controlling seismic response of the dynamic system and their combination for TSD braced at a specified angle, may lead to optimal seismic response control for given seismic excitation. This condition forms basis for developing optimization problem formulation. Requirement of relatively higher sling length for TSD may offer practical difficulties and can be seen as a constraint for the

proposed TSD. However, this can be negated using TSD in combination with other compatible passive control devices which is beyond the scope of present study.

It is observed that TSD efficiently controls seismic response across all categories of dynamic systems considered in the present study. Flexible - and while moderately stiff systems utilize damping component stiff systems exploit stiffness component of TSD to yield seismic response control of the dynamic system. The said results can be followed from Equation (11) as cross-sectional area of SMA slings contribute stiffness component and sling length contributes damping component of the passive damper force.

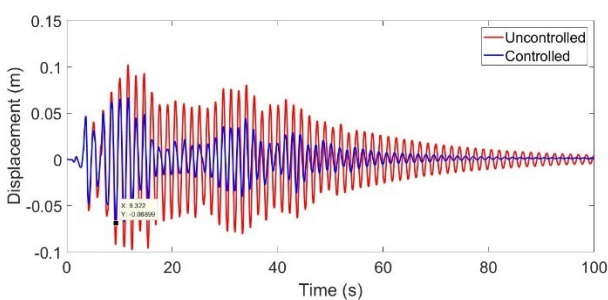


Figure 11a

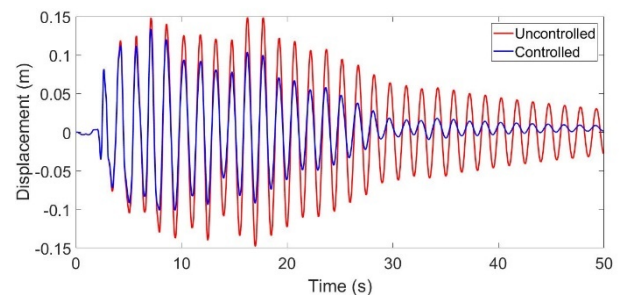


Figure 11c

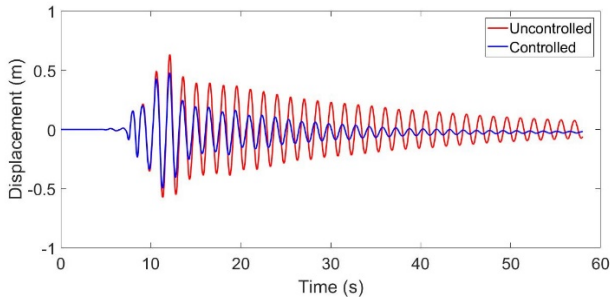


Figure 11b

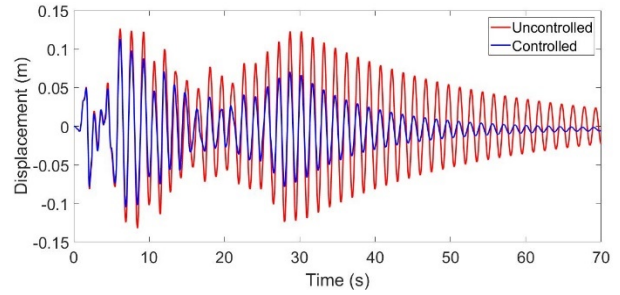


Figure 11d

Figure 11 Comparison of uncontrolled and controlled displacement response of flexible dynamic system ( $T_n=1.5s$ ) subjected to (a) Taft (b) Kobe (c) Loma Prieta and (d) El Centro seismic excitation

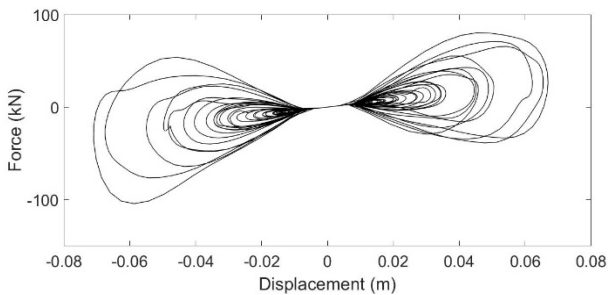


Figure 12a

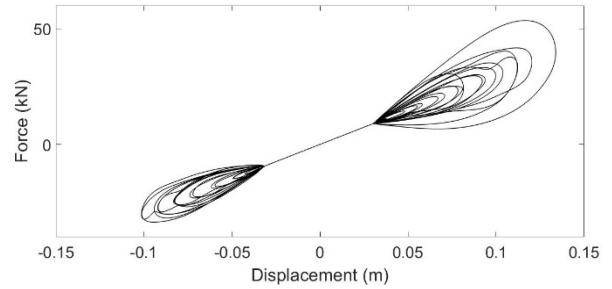


Figure 12c

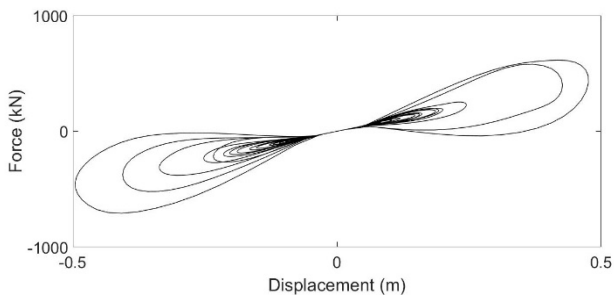


Figure 12b

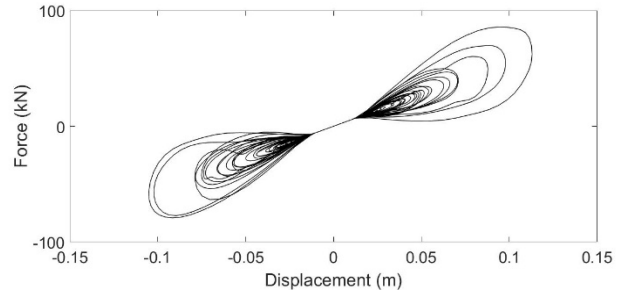


Figure 12d

Figure 12 Passive damper force vs displacement of flexible dynamic system ( $T_n=1.5s$ ) subjected to (a) Taft (b) Kobe (c) Loma Prieta and (d) El Centro seismic excitations

Uncontrolled and controlled displacement response of the system is shown in Figure 11a to Figure 11d for each seismic excitation considered in the study for dynamic system with  $T_n=1.5s$ . It is seen that peak displacements occur at 11.62s and 9.32s for Taft excitation; 12.12s and 11.24s for Kobe excitation; 16.24s and 7.01s for Loma Prieta excitation and 8.42s and 6.16s for El Centro excitation, respectively. Early occurrence of peak displacement for controlled system vis-a-vis uncontrolled system falls in line with the results reported by similar studies in the literature.

It is seen that TSD fitted controlled system ( $T_n=1.5s$ ) shows reduction in displacement time history across all seismic excitations considered for the present study. Reduction in displacement time histories for other two dynamic systems are also observed.

Damper force vs displacement relation for TSD fitted with the above-mentioned system subjected to various seismic excitations is shown in Figure 12a to

Figure 12d. Damper force shows hysteretic nature ensuring energy dissipation and is realized mostly in first and third quadrant. It is evident that TSD is mostly driven by damping component under strong ground motion and thus results into broader hysteretic loop. Hysteretic loop of TSD flattens for strain, in SMA tension slings, below transformation strain of super-elastic SMA wire.

Variation in Martensite Volume Fraction (MVF) and damping ratio ( $\zeta$ ) at each instant for Taft seismic excitation are represented in Figure 13, where MVF is determined through Tanaka model of SMA. Instantaneous damping ratio is evaluated following Equation (14) considering area of hysteresis loop at each instant for TSD fitted to flexible dynamic system.

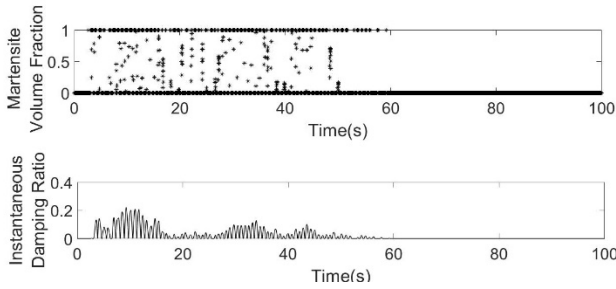


Figure 13 Variation of Instantaneous Damping Ratio and martensite volume fraction for Taft seismic excitations flexible dynamic system

MVF assumes lower bound value of ‘0’ indicating austenite phase and upper bound value representing transformation phase – martensite of SMA wire. Figure 13 also depicts instantaneous damping offered by passive TSD, due to frequent phase transformation in super-elastic SMA wire, contributing to supplemental damping than inherent damping possessed by the system. Evidently, damping ratio of the system will not increase if phase transformation does not take place in SMA sling and thus contribution of SMA be limited to offer stiffness to the system resembling bracing component of structural system. Other research studies have introduced concept of pre-straining of SMA to ensure phase transformation of SMA so that super-elastic properties of SMA are utilized.

Instantaneous damping ratio realized by TSD under Kobe, Loma Prieta and El Centro excitation are evaluated in Figure 14 a, b & c, respectively where maximum instantaneous damping ratio ranges between 22.08% to 0.28% of the critical damping.

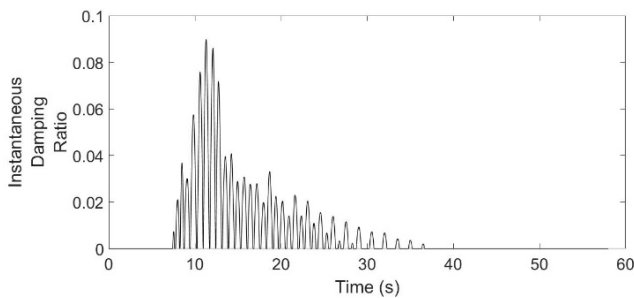


Figure 14 a

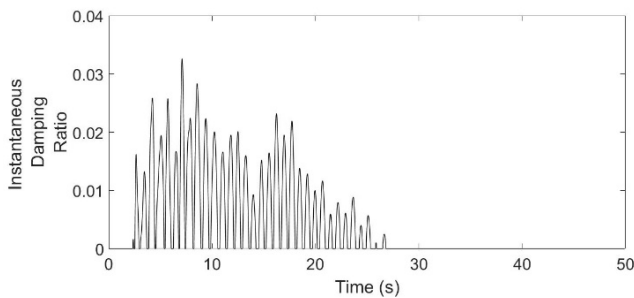


Figure 14 b

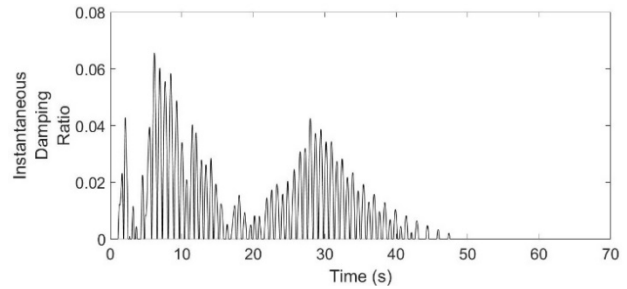


Figure 14 c

Figure 14 Variation of instantaneous damping ratio for flexible system subjected to a) Kobe b) Loma Prieta and c) El Centro seismic excitation

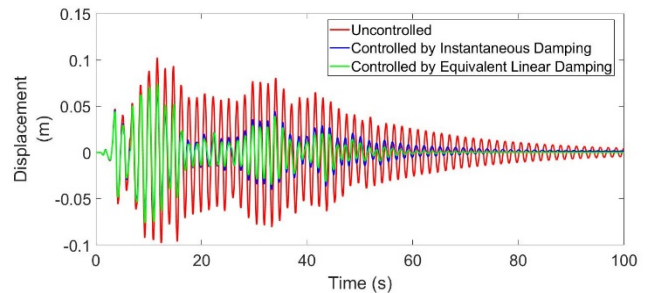


Figure 15 comparison of displacement response for uncontrolled system, controlled system with instantaneous damping model and controlled system by equivalent linear elastic viscous damping model (Ghodke & Jangid, 2016)

Figure 15 shows comparison between displacement response of controlled SDOF system with equivalent piece-wise linear elastic viscous model (proposed in the study) and equivalent linear elastic viscous model of Ghodke and Jangid (2016) vis-à-vis uncontrolled dynamic system for Taft seismic excitations. It indicates that equivalent linear viscous damping model of Ghodke and Jangid yields better results as compared to present study as model implements constant and maximum damping offered by SMA.

#### 4 CONCLUSIONS

Present paper proposes a SMA based Tension Sling Damper (TSD) for passive seismic response control of the dynamic system. Mechanism and features of proposed TSD are summarized. SMA sling is modelled as equivalent piece-wise linear elastic viscous damping model to map non-linear stress-strain behaviour of SMA characterized by unified Tanaka model. A building structure represented as discrete SDOF dynamic system is simulated for pulse type and strong ground motion type seismic excitations. Response parameters – peak and rms performance indices, peak damper force and maximum damping ratio are evaluated for controlled system fitted with TSD. Substantial reduction in peak and rms displacement response

of the dynamic system is achieved by varying design parameters – cross-sectional area and SMA sling length for each seismic excitation. Peak and rms acceleration, of the system are found to reduce moderately. Dynamic system yields better seismic response control, when the strain induced in super-elastic SMA wire ranges between 3 to 4.5% for all seismic excitations except Taft excitation where effective control is seen for strain of the order 6% due to higher frequency content. Out of three dynamic systems, moderately stiff system ( $T_n=0.7s$ ) yields best seismic response control with TSD. For stiff systems, instantaneous ratio realized by TSD is quite low and seismic control is achieved due to stiffness component of the damper force, leading to ineffective seismic response control. Thus, one might have to apply pre-strain to SMA sling to derive desirable seismic response.

Present study suggests that proposed TSD works effectively with flexible and moderately stiff system due to super-elastic properties of SMA undergoing substantial strain under seismic excitations. Requirement of relatively higher sling length for seismic excitations like Kobe reveals that such solution may be practically difficult and imposes a limitation for the use of TSD. However, proposed TSD may be used with other compatible passive device to control the seismic response effectively. Optimization techniques may be employed to derive diameter and sling length for TSD with objective function on displacement and/or acceleration response.

## 5 REFERENCES

- Bertrand, E., Castany P., and Glorient, T., “Investigation of the martensitic transformation and the damping behavior of a superelastic Ti-Ta-Nb alloy”, *Acta Materialia*, 2013, Vol. 61, No. 2, 511-518.
- Buehler, W., and Wiley, R., “Nickel based alloys”, 1961; patent US3174851A
- Caughey, T., “Sinusoidal excitation of a system with bilinear hysteresis”, *ASME Journal of Applied Mechanics*, 1960, Vol. 27, No. 4, 1-4.
- DesRoches, R., McCormick, J. and Delemont, M., “Cyclic properties of super elastic shape memory alloys wire and bars”, *Journal of Structural Engineering*, 2004, Vol. 1, No. 38, 39-46.
- Dolce, M., Cardone, D., Ponzo, F., and Valente, C., “Shaking table tests on reinforced concrete frames without and with passive control systems”, *Earthquake Engineering and Structural Dynamics*, 2005, Vol. 34, 1687-1717.
- Ghodke, S., and Jangid, S., “Equivalent linear elastic-viscous model of shape memory alloy for isolated structures”, *Advances in Engineering Software*, 2016, Vol. 99, No. 22, 1-8.
- Graesser, E. and Cozzarelli, F., “Shape-Memory Alloys as new materials for seismic isolation”, *Journal of Engineering Mechanics*, 1991, Vol. 117, No. 11, 2590-608.
- Gur, S., Mishra S. and Roy K. “Stochastic seismic response of building with super-elastic damper”, *Mechanical Signal Processing*, 2016, Vol 72-73, 642-659.
- Han, Y., Li, Q. S., Li, A. Q., Leung, A. Y. T., and Lin, P., “Structural vibration control by shape memory alloy damper”, *Earthquake Engineering and Structural Dynamics*, 2003, Vol. 32, 483-494.
- Hartl, D. J., and Lagoudas, D. C., “Thermomechanical characterization of shape memory alloy material, Shape Memory Alloys: modelling and engineering Applications”, Springer Science, 2008; 53-119.
- Jani, J. M., Leroy, M., Subik, A., and Gibson, M., “A review of shape memory alloy research, applications and opportunities”, *Materials and Design*, 2014, Vol. 56, 1078-1114.
- Jansen, L. M., and Dyke, S. J., “Semi-active control strategies for MR dampers: A Comparative Study, *Journal of Engineering Mechanics*”, 1999, vol 126, No. 8, 795-803.
- Kumar, P. K., Lagoudas, D. C. (ed), “Introduction to shape memory alloys, Shape Memory Alloys: Modelling and Engineering Applications”, Springer Science, 2008, 1-15.
- Kurdjumov, G. V., and Khandros, L. G., “The thermoelastic behaviour of the martensitic phase of Au-Cd alloys”, *Doklady Akademii Nauk*, 1949, Report SSSR 66, 211-213
- Lobo, P., Almeida, J., and Guerreiro, L., “Semi-active damping device based on superelastic shape memory alloys”, *Structures*, 2015, Vol. 3, 1-12
- McCormick, J., DesRoches, R., Fugazza, D., and Auricchio, F., “Seismic vibration control using superelastic shape memory alloys”, *Journal of Engineering Materials and Technology*, 2006, Vol. 128, 294-301.
- Miller, D. J., Fahnstock, L., and Eatherton, M., “Development and experimental validation of a Nickel - Titanium shape memory alloy self centering and buckling restrained braces”, *Engineering Structures*, 2012, Vol. 40, 288-298.
- Morais, J., Morais, P., Santos, C., Campos Costa, A., and Candéias, P., “Shape memory alloy based dampers for earthquake response mitigation”, *Structural Integrity Procedia*, 2017; Vol. 5, 705-712.
- Mortazavi, S. M. R., Ghassemieh, M., and Motahari, S.A., “Seismic control of steel structures with shape memory alloys”, *International Journal of Automation and Control Engineering*, 2013, Vol. 2, No. 1, 28-34.
- Ohtori, Y., Christensen, R. E., Spencer, B. F. Jr., and Dyke, S. J., “Benchmark problems for seismically excited nonlinear buildings”, *Journal of Engineering Mechanics*, 2004, Vol. 130, No. 4, 366-385.

- Parulekar, Y. M., Ravi Kiran, A., Reddy, G. R., Singh, R. K., and Vaze, K. K., "Shake table tests and analytical simulations of a steel structure with shape memory alloy dampers", *Smart Materials and Structures*, 2014, Vol. 23, 1-12.
- Purohit, S. P., and Chandiramani, N. K., "Optimal static output feedback control of a building using an MR Damper", *Structural Control and Health Monitoring*, 2010, Vol. 18, No. 8, 852-868.
- Seelecke, S., Heintze, O., and Masuda, A., "Simulation of earthquake-induced structural vibrations in systems with SMA damping element", *Proceedings of the SPIE Smart Structures & Materials*, 2002, 4697, 1-8.
- Sherif, M., and Ozbulut, O., "Tensile And super-elastic fatigue characterization Of NiTi shape memory cables", *Smart Materials and Structures*, 2018, Vol. 27, 1-13.
- Song, G., Ma, N., and Li, H. N., "Applications of shape memory alloys in civil structures", *Engineering Structures*, 2006, Vol. 28, 1266-1274.
- Soong, T. T., and Spencer B. F., "Supplementary energy dissipation: state-of-the-art and state-of-the-practice", *Engineering Structures*, 2002, Vol. 24, 243– 259.
- Spencer, B. F., and Nagarajaiah, S., "State of the art structural control", *Journal of Structural Engineering*, 2003, Vol. 129, 845-856.-
- Symans, M. D., Charney, F. A., Whittaker, A. S., Constantinou, M. C., Kircher, C. A., Johnson, M. W., and McNamara, R. J., "Energy dissipation systems for seismic applications: current practice and recent developments", *Journal of Structural Engineering*, 2008, Vol. 134, No. 1, 4-21.
- Tanaka, K., "A thermomechanical sketch of shape memory effect: one-dimensional tensile behaviour", *Research Mechanical*, 1986, Vol. 18, 251-263
- Xu Y.L., Qu W.L., and Ko J. M., "Seismic response control of frame structures using magnetorheological/electrorheological dampers", *Earthquake Engineering Structural Dynamics*, 2000, Vol. 29-5, 557-575.
- Zhang, Y., and Zhu, S., "A shape memory alloy-based reusable hysteretic damper for seismic hazard Mitigation", *Smart Materials and Structures*, 2007, Vol.16, 1603-1613.